

Unraveling neutrino parameters with a magical beta-beam experiment at INO

Sanjib Kumar Agarwalla^{*,†,a}, Sandhya Choubey^{*,b}, Amitava Raychaudhuri^{*,†,c}

**Harish-Chandra Research Institute,
Chhatnag Road, Jhansi, Allahabad 211019, India*

*†Department of Physics, University of Calcutta,
92 Acharya Prafulla Chandra Road, Kolkata 700009, India*

ABSTRACT

We expound in detail the physics reach of an experimental set-up in which the proposed large magnetized iron detector at the India-based Neutrino Observatory (INO) would serve as the far detector for a so-called beta-beam. If this pure ν_e and/or $\bar{\nu}_e$ beam is shot from some source location like CERN such that the source-detector distance $L \simeq 7500$ km, the impact of the CP phase δ_{CP} on the oscillation probability and associated parameter correlation and degeneracies are almost negligible. This “magical” beta-beam experiment would have unprecedented sensitivity to the neutrino mass hierarchy and θ_{13} , two of the missing ingredients needed for our understanding of the neutrino sector. With Lorentz boost $\gamma = 650$ and irrespective of the true value of δ_{CP} , the neutrino mass hierarchy could be determined at 3σ C.L. if $\sin^2 2\theta_{13}(\text{true}) > 5.6 \times 10^{-4}$ and we can expect an unambiguous signal for θ_{13} at 3σ C.L. if $\sin^2 2\theta_{13}(\text{true}) > 5.1 \times 10^{-4}$ independent of the true neutrino mass hierarchy.

^a email: sanjib@mri.ernet.in

^b email: sandhya@mri.ernet.in

^c email: raychaud@mri.ernet.in

1 Introduction

Neutrino physics has entered the precision era, with the thrust now shifting to detailed understanding of the structure of the neutrino mass matrix, accurate reconstruction of which would shed light on the underlying new physics that gives rise to neutrino mass and mixing. The full mass matrix is given in terms of nine parameters, the three neutrino masses, the three mixing angles and the three CP violating phases. Neutrino oscillation experiments are sensitive to only two mass squared differences, all the three mixing angles and the so-called Dirac CP violating phase. The remaining parameters, comprising of the absolute neutrino mass scale and the two so-called Majorana phases, have to be determined elsewhere. We already have very good knowledge on the two mass squared differences and two of the three mixing angles. Results from solar neutrino experiments [1], which have been collecting data for more than four decades have now culminated in choosing the Large Mixing Angle (LMA) solution. The latest addition to this huge repertoire of experimental data is the result from the on-going Borexino experiment [2], and this result is consistent with the LMA solution. This conclusion from solar neutrino experiments has been corroborated independently by the KamLAND reactor antineutrino experiment [3, 4], and a combined analysis of the solar and KamLAND data gives as best-fit¹ $\Delta m_{21}^2 = 7.6 \times 10^{-5} \text{ eV}^2$ and $\sin^2 \theta_{12} = 0.32$ [4, 5]. The other mass squared difference Δm_{31}^2 and mixing angle θ_{23} are now pretty well determined by the zenith angle dependent atmospheric ν_μ data in SuperKamiokande [6] and the long baseline experiments K2K [7] and MINOS [8]. The combined data from the atmospheric and long baseline experiments have pinned down $|\Delta m_{31}^2| = 2.4 \times 10^{-3} \text{ eV}^2$ and $\sin^2 2\theta_{23} = 1$.

Despite these spectacular achievements, a lot of information is still required to complete our understanding of the neutrino sector. While the solar neutrino data have confirmed that $\Delta m_{21}^2 > 0$ at a C.L. of more than 6σ , we still do not know what is the sign of Δm_{31}^2 . Knowing the ordering of the neutrino masses is of prime importance, because it dictates the structure of the neutrino mass matrix, and hence could give vital clues towards the underlying theory of neutrino masses and mixing. Knowing the $\text{sgn}(\Delta m_{31}^2)$ could have other far-reaching phenomenological consequences. For instance, if it turns out the $\Delta m_{31}^2 < 0$ and yet neutrino-less double beta decay is not observed even in the very far future experiments, that would be a strong hint that the neutrinos are not Majorana particles (see for *e.g.* [9] and references therein). Also, our knowledge on the third mixing angle θ_{13} is restricted to an upper bound of $\sin^2 \theta_{13} < 0.04$ from the global analysis of all solar, atmospheric, long baseline and reactor data, including the CHOOZ [10] results in particular. Non-zero θ_{13} brings in the possibility of large Earth matter effects [11, 12, 13] for GeV energy accelerator neutrinos travelling over long distances. Effect of matter on neutrino oscillations depends on the $\text{sgn}(\Delta m_{31}^2)$ and is opposite for neutrinos and antineutrinos. For a given $\text{sgn}(\Delta m_{31}^2)$ it enhances the oscillation probability in one of the channels and suppresses it in the other. Therefore, comparing the neutrino signal against the antineutrino signal in very long baseline experiments gives us a powerful tool to determine $\text{sgn}(\Delta m_{31}^2)$. A non-zero value of this mixing angle would also open up the possibility of detecting CP violation in the neutrino sector.

Tremendous effort is underway to determine θ_{13} , the CP phase δ_{CP} and $\text{sgn}(\Delta m_{31}^2)$ using long baseline experiments [14, 15, 16, 17]. Future programs involving accelerator based neutrino beams

¹We use a convention where $\Delta m_{ij}^2 = m_i^2 - m_j^2$.

include among others the T2K [14], NO ν A [15], Superbeams, beta-beams and Neutrino Factories [17]. In earlier papers [18, 19] we have proposed and expounded the possibility of measuring to a very high degree of accuracy the mixing angle θ_{13} and $\text{sgn}(\Delta m_{31}^2)$ aka, the neutrino mass hierarchy², in an experimental set-up where a pure and intense ν_e and/or $\bar{\nu}_e$ beam is shot from CERN to the India-based Neutrino Observatory (INO) [20]. This pure and intense source of ν_e and/or $\bar{\nu}_e$ flux could be the so-called beta-beam [21], which is created when fully ionized and highly accelerated radioactive ions beta decay in the straight sections of a ring, where they are circulated and stored, after being produced, collected, bunched and accelerated. A large magnetized iron calorimeter (ICAL) is expected to come-up soon at the INO facility in India. Since the energy threshold of this detector would be at least 1 GeV, the beta-beam should necessarily be a multi-GeV beam. While the most widely discussed source ions for beta-beams, ^{18}Ne and ^6He , need very large values of the Lorentz boost to reach multi-GeV energies [18], alternative ions with larger end-point energy, such as ^8B and ^8Li , can be used with reasonable acceleration. While the most discussed design for the beta-beam set-up [22] needs modest Lorentz boosts, it suffers from the effect of the so-called “parameter degeneracies” [23, 24, 25] giving rise to eight-fold degenerate “clone solutions” [26]. A very big advantage that the CERN-INO beta-beam experiment would have is that at the baseline of 7152 km, the δ_{CP} dependent terms (almost) drop out from the expression for the $\nu_e \rightarrow \nu_\mu$ oscillation probability. As a result, this experiment is free of two of the three degeneracies [26, 27, 28]. In addition, large energies and the large distance involved allows the neutrino to pick up near-resonant matter effects, enhancing the oscillation probability which can thereby compensate to a great extent the reduction of the neutrino flux due to the $1/L^2$ factor [19]. This makes the CERN-INO beta-beam set-up almost magical for determining $\text{sgn}(\Delta m_{31}^2)$ and θ_{13} .

In [19] we studied the physics potential of this experimental set-up when we run the beta-beam in *only one polarity* for five or ten years. That is, we probed the sensitivity of the experiment to $\text{sgn}(\Delta m_{31}^2)$ and θ_{13} using *only* the ν_e ($\bar{\nu}_e$) beam for five years running with 1.1×10^{18} (2.9×10^{18}) useful ion decays per year. In this paper we extend our analysis by including data from *both* the neutrino and antineutrino run of this beta-beam experimental set-up. We demonstrate how adding data from both polarities serves to strengthen precisely those regions where the individual ones are less powerful and thus significantly enhances the mass hierarchy sensitivity of the experiment. As a further refinement, we analyse the full spectral data expected in the CERN-INO beta-beam set-up. We present and compare results from the rates-only analysis against results from the analysis where we incorporate the full spectrum. For θ_{13} measurement, we consider two scenarios: (i) when there are no ν_μ (or $\bar{\nu}_\mu$) events in the detector and (ii) when we see a signal in the detector. In the former case we present the 3σ upper bound on $\sin^2 2\theta_{13}$ expected from the null results. We call this the “ $\sin^2 2\theta_{13}$ sensitivity reach” of the experiment. In the latter case, we first study the range of “true” values³ of $\sin^2 2\theta_{13}(\text{true})$ for which the experiment would be able claim to have seen a signal at the 3σ C.L. This is termed as the “ $\sin^2 2\theta_{13}(\text{true})$ discovery reach” of the experiment. Finally, for a non-zero signal at the detector, we study how precisely $\sin^2 2\theta_{13}$ can be determined with 5

²What we usually refer to as the neutrino mass hierarchy is really the neutrino mass ordering. Therefore, our discussion and results are equally relevant for a quasi-degenerate neutrino mass spectrum as they are for hierarchical and inverted hierarchical spectra.

³Throughout this paper we denote true value of the parameters by putting “(true)” in front of them.

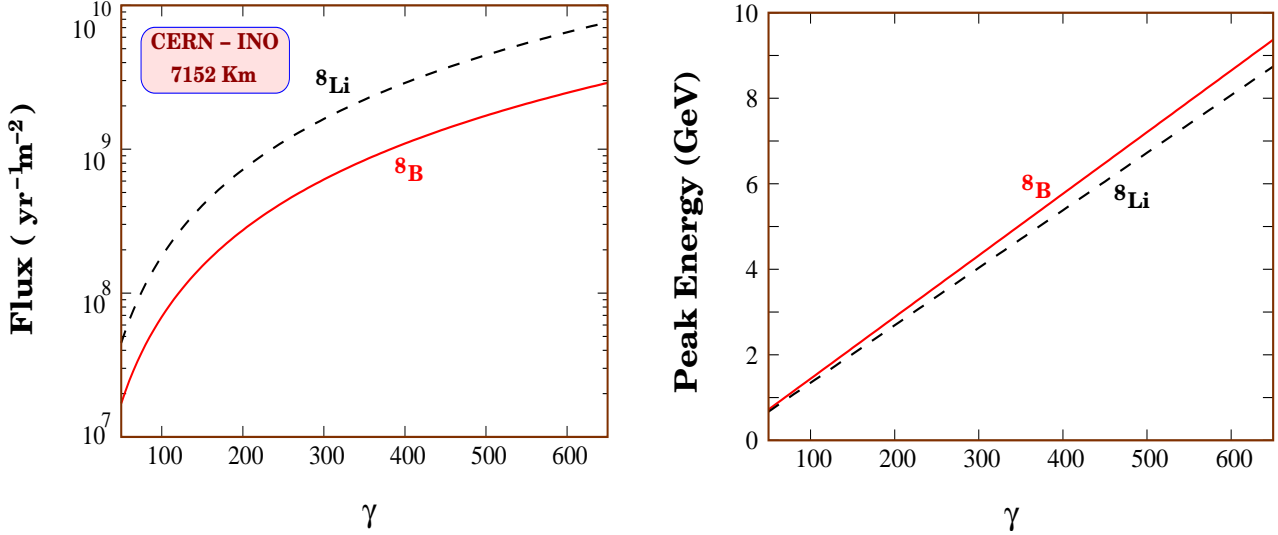


Figure 1: Left panel shows the total flux in $\text{yr}^{-1}\text{m}^{-2}$ expected at INO, as a function of the Lorentz factor γ . The solid (dashed) line corresponds to ^8B (^8Li) and we have assumed 1.1×10^{18} (2.9×10^{18}) useful ions decays per year. Right panel shows the energy at which the flux peaks, as a function of γ .

years of combined neutrino and antineutrino run. In our earlier paper [19], we had given all results assuming that $\delta_{CP}(\text{true}) = 0$. The hierarchy and θ_{13} measurement sensitivities however depend on the value of $\delta_{CP}(\text{true})$. In this paper we find the physics reach of the CERN-INO beta-beam set-up for all possible values of $\delta_{CP}(\text{true}) = 0$ and show the best and worst possible physics reach. We also study the impact of changing the number of useful ion decays in the straight sections of the beta-beam storage ring and compare the dependence of the sensitivity on the number of ion decays and the Lorentz boost γ .

For all results presented in this paper, we use the full PREM Earth matter density profile [30] for simulating the prospective data. When we fit this simulated data, we allow for a 5% uncertainty in the PREM profile and take it into account by inserting a prior and marginalizing over the density normalization. We also study the impact of changing the Earth matter density by $\pm 5\%$ in the data itself. We also study the impact of changing the energy threshold of the detector and the background rejection factor. In our analysis here we also allow the parameters Δm_{21}^2 and $\sin^2 \theta_{12}$ to vary arbitrarily in the fit.

We begin by providing a brief overview of the proposed experimental set-up, the expected event rate, and the importance of the magic baseline in section 2. In section 3, we give our results on the sensitivity of the CERN-INO beta-beam set-up to the neutrino mass hierarchy. In section 4, we discuss the potential of measuring/constraining θ_{13} . We end with our conclusions in section 5. The details of our numerical code and analysis procedure are relegated to an Appendix.

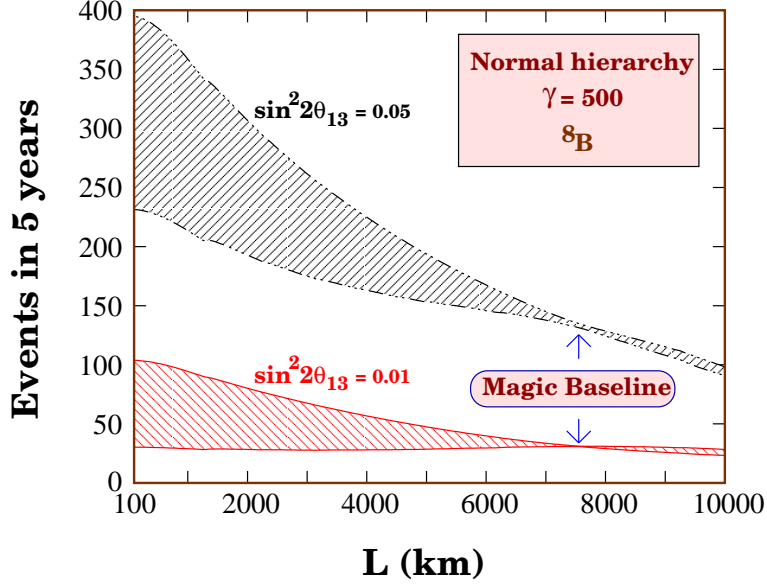


Figure 2: Total number of expected events in five years as a function of the baseline L for the ${}^8\text{B}$ source with $\gamma = 500$ and for two values of $\sin^2 2\theta_{13}$ and assuming that the normal hierarchy is true. The hatched areas show the expected uncertainty due to the CP phase.

2 The CERN-INO beta-beam Experimental Set-up

Very pure and intense ν_e and/or $\bar{\nu}_e$ beams can be produced by the decay of highly accelerated radioactive beta unstable ions, circulating in a storage ring. This is what is called a “beta-beam” and was first proposed by Piero Zucchelli [21]. Since the flux spectrum is determined entirely by the end-point energy of the parent ions and the Lorentz boost provided by the acceleration, it is almost free of systematic uncertainties. The flux normalization is determined by the number of useful ion decays in the straight section of the beam. The selection of the beta unstable parent ion is determined by a variety of factors essential for efficiently producing, bunching, accelerating and storing these ions in the storage ring. Among the candidate ions discussed in the literature, the ones which have received most attention so far are the ${}^{18}\text{Ne}$ and ${}^6\text{He}$ ions for producing the ν_e and $\bar{\nu}_e$ beams respectively [22, 31, 32, 33, 34, 35]. Both these ions have a similar end-point energy which is about 4 MeV in the parent ion’s rest frame. Two other candidates, ${}^8\text{B}$ and ${}^8\text{Li}$, as source ions for ν_e and $\bar{\nu}_e$ beams respectively, have been recently shown to be viable [36, 37, 38, 39, 40]. The advantage that these ions have over ${}^{18}\text{Ne}$ and ${}^6\text{He}$ is their larger end-point energies, which is higher by a factor of more than 3. Therefore, for the same Lorentz boost factor, we expect the resultant ${}^8\text{B}$ and ${}^8\text{Li}$ beams to be about 3 times higher in energy compared to the ${}^{18}\text{Ne}$ and ${}^6\text{He}$ beams. We refer the reader to Table 1 of our earlier paper [19] for the full details about characteristics of the four beta-beam candidate ions.

These large beta decay end-point energy ions are particularly important for the CERN-INO

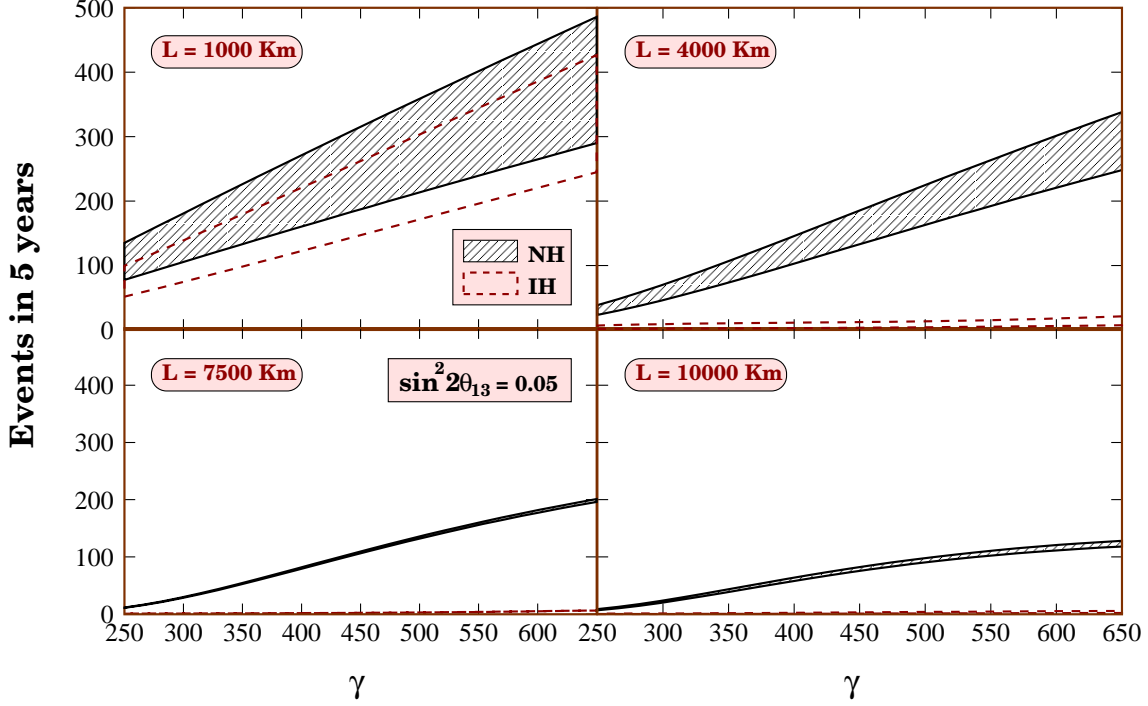


Figure 3: Total number of events as a function of γ for the 8B source, for different values of L are shown in the four panels. The black hatched area shows the uncertainty range due to the CP phase when NH is true, while the area between the maroon dashed lines shows the corresponding uncertainty when IH is true. For all cases we assume $\sin^2 2\theta_{13} = 0.05$.

beta-beam experimental set-up discussed in [18, 19], where the beta-beam from CERN is shot to a magnetized iron detector at the India-based neutrino observatory (INO). The INO will be located in southern India, close to the city of Bangalore. The CERN to INO distance corresponds to 7152 km, which is tantalizingly close to the “magic baseline” [27, 28] (see also [29]). Being free of the problem of parameter degeneracies [23, 24, 25, 26], the magic baseline is known to be particularly useful for measuring the mixing angle θ_{13} and $\text{sgn}(\Delta m_{31}^2)$. The concept of the magic baseline can be very easily understood by looking at the approximate expression of $P_{e\mu}$, where the conversion probability is expanded in the small parameters θ_{13} and $\alpha \equiv \Delta m_{21}^2 / \Delta m_{31}^2$, keeping only terms up to second order in these small parameters. This expression for the “golden channel” [41] probability is given as [41, 42]

$$\begin{aligned}
 P_{e\mu} \simeq & \sin^2 \theta_{23} \sin^2 2\theta_{13} \frac{\sin^2[(1 - \hat{A})\Delta]}{(1 - \hat{A})^2} \\
 & + \alpha \sin 2\theta_{13} \sin 2\theta_{12} \sin 2\theta_{23} \sin \delta_{CP} \sin(\Delta) \frac{\sin(\hat{A}\Delta)}{\hat{A}} \frac{\sin[(1 - \hat{A})\Delta]}{(1 - \hat{A})}
 \end{aligned}$$

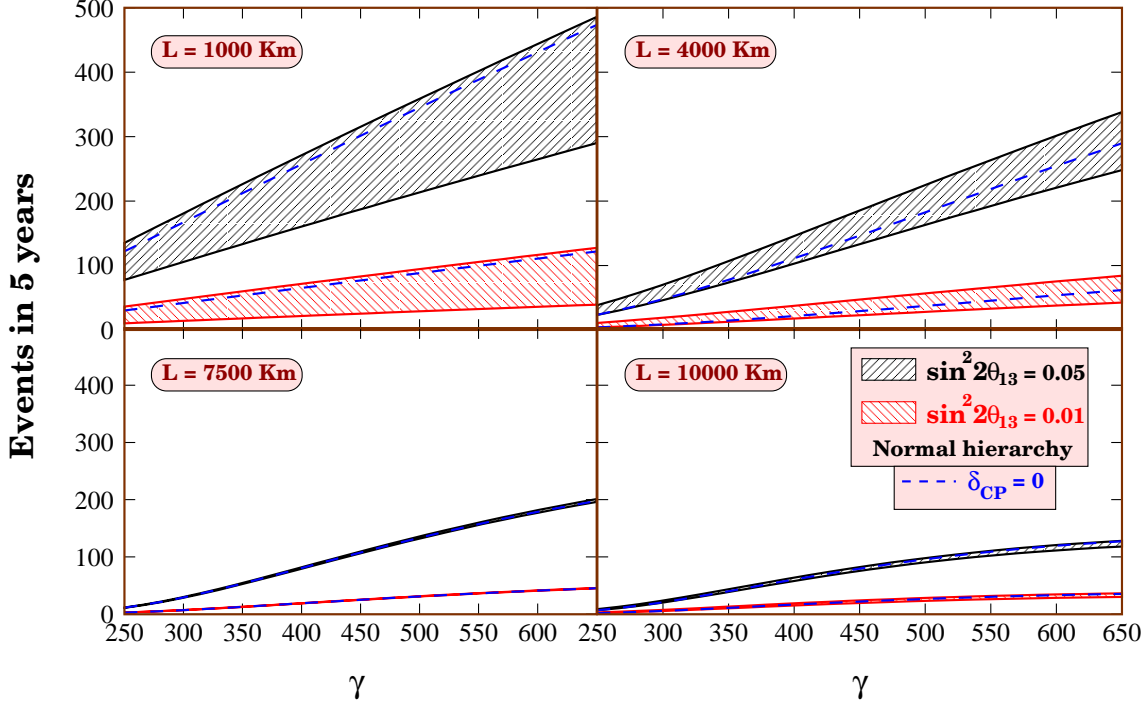


Figure 4: Total number of events as a function of γ for the 8B source, for different values of L are shown in the four panels. The black hatched area shows the uncertainty range in the events due to CP phase when $\sin^2 2\theta_{13} = 0.05$, while the red hatched area shows the corresponding uncertainty when $\sin^2 2\theta_{13} = 0.01$. For all cases we assume NH to be true.

$$\begin{aligned}
& + \alpha \sin 2\theta_{13} \sin 2\theta_{12} \sin 2\theta_{23} \cos \delta_{CP} \cos(\Delta) \frac{\sin(\hat{A}\Delta)}{\hat{A}} \frac{\sin[(1-\hat{A})\Delta]}{(1-\hat{A})} \\
& + \alpha^2 \cos^2 \theta_{23} \sin^2 2\theta_{12} \frac{\sin^2(\hat{A}\Delta)}{\hat{A}^2},
\end{aligned} \tag{1}$$

where

$$\Delta \equiv \frac{\Delta m_{31}^2 L}{4E}, \quad \hat{A} \equiv \frac{A}{\Delta m_{31}^2}, \tag{2}$$

where $A = \pm 2\sqrt{2}G_F N_e E$ is the matter potential, N_e being the electron number density inside the earth and G_F the Fermi constant, the $+$ sign refers to neutrinos while the $-$ to antineutrinos. In Eq. (1) the second term has the CP violating part. The CP phase δ_{CP} is positive for neutrinos and negative for antineutrinos and therefore the $\sin \delta_{CP}$ term changes sign. The third term, though δ_{CP} dependent, is CP conserving, while the fourth term is independent of θ_{13} as well as δ_{CP} . If there exists a baseline L for which the condition

$$\sin(\hat{A}\Delta) = 0 \tag{3}$$

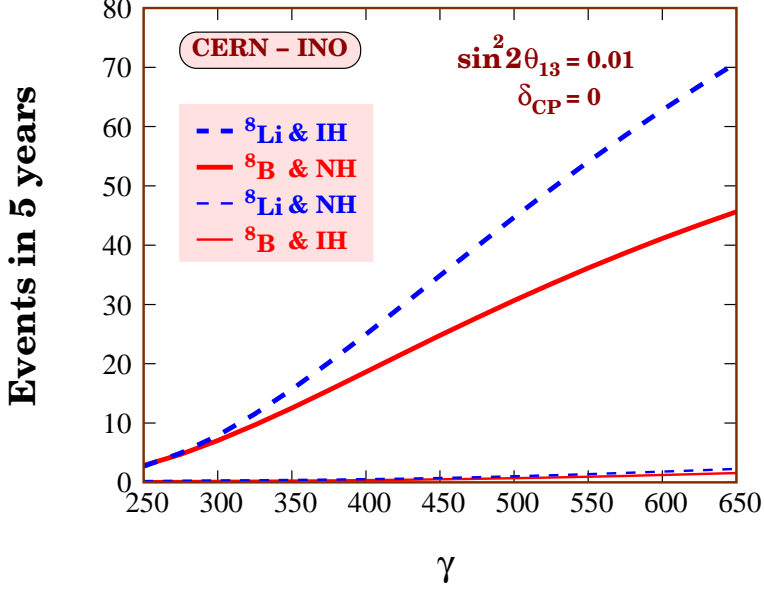


Figure 5: Total number of events as a function of γ for the ${}^8\text{B}$ (solid lines) and the ${}^8\text{Li}$ (dashed lines) sources. Results for both normal and inverted hierarchies are shown.

holds, then the second, third and fourth terms in Eq. (1) drop out and one is left with just the first term. In particular, we see that all δ_{CP} dependent terms go away at this magic baseline. Therefore, this experimental set-up is free of two of the three parameter degeneracies, providing us with a firm bedrock for determining θ_{13} and the mass hierarchy [27, 19]. It turns out that for the PREM Earth matter density profile, the condition given by Eq. (3) is satisfied for $L \simeq 7500$ km. In [19] we also stressed the point that for this very long baseline, neutrinos would also pick up large, and possibly near-resonant, matter effects. Largest enhancement of oscillations due to matter effects of course comes about when the product of the mixing angle term in matter and the $(\Delta m_{31}^2)^M$ driven oscillatory term is the largest [43, 44]. For the CERN-INO baseline of 7152 km, the probability for largest conversion is expected for $E \simeq 6$ GeV, for $\sin^2 2\theta_{13} = 0.01$ and $\Delta m_{31}^2 = 2.5 \times 10^{-3} \text{ eV}^2$.

The ICAL detector, which will be a 50 kton magnetized iron calorimeter, will be built at INO [20]. There is a possibility that the detector mass might be increased to 100 kton at a later stage. The approved design of the detector comprises of 6 cm iron slabs interleaved with 2 cm thick glass Resistive Plate Chambers (RPC), which would serve as the active detector elements for ICAL. The iron will be magnetized by an external field of about 1 Tesla, giving the detector charge identification capability. The detection efficiency of ICAL after cuts is expected to be about 80% and energy threshold would be about 1 GeV. In what follows, we will use an energy threshold of 1.5 GeV for our main results. However, we will also show the impact of changing the threshold. The energy resolution of the detector is expected to be reasonable and we assume that the neutrino energy will be reconstructed with an uncertainty parameterized by a Gaussian energy resolution

function with a HWHM $\sigma_E = 0.15E$, where E is the energy of the neutrino. We will present and compare the sensitivity of this experimental set-up with and without the full spectral analysis. Details of our numerical approach can be found in [19] and in the Appendix.

In the left panel of Fig. 1 we show the energy integrated total number of neutrinos in units of $yr^{-1}m^{-2}$ arriving at INO, as a function of the Lorentz boost γ . The solid (dashed) line corresponds to 8B (8Li) and we have assumed 1.1×10^{18} (2.9×10^{18}) useful ion decays per year⁴. Throughout this paper we have assumed that the detector is aligned along the axis of the beam. The figure shows that the energy integrated flux arriving at the detector increases almost quadratically with γ . Note that with the same accelerator, the Lorentz boost acquired by 8B is 1.67 times larger than that by 8Li , determined by the charge to mass ratios of the ions. The right panel of Fig. 1 depicts the energy at which the flux peaks, as a function of the Lorentz boost γ . It turns out that this peak energy is roughly half the maximum energy of the beam, which is given as $E_{\max} \simeq 2(E_0 - m_e)\gamma$.

In Fig. 2 we show the number of events expected in five years as a function of the baseline L , if we run the experiment in the neutrino mode with $\gamma = 500$. A similar figure is expected for the antineutrino beam. The upper black hatched area shows the events for $\sin^2 2\theta_{13} = 0.05$ and the lower red hatched area corresponds to $\sin^2 2\theta_{13} = 0.01$. For each baseline L , the range covered by the hatched area shows the uncertainty in the expected value of the number of events due to the completely unknown δ_{CP} , which could take any value from 0 to 2π . The baseline L where the width of this band reduces to (almost) zero is the magic baseline. We see from the figure that the magic baseline appears at about $L \simeq 7500$ km. Note that while for $\sin^2 2\theta_{13} = 0.01$ the magic baseline is very clearly defined with the CP dependence going completely to zero, for the higher value of $\sin^2 2\theta_{13}$ of 0.05, the “magic” is not complete. The reason for this anomaly can be traced to the fact that Eq. (1) was derived for only very small values of θ_{13} . For larger values of this angle, higher order terms become important. These terms might depend on δ_{CP} and remain non-zero even at the magic baseline.

In Figs. 3 and 4 we show the impact of the magic baseline on the mass hierarchy and θ_{13} sensitivity respectively. In each of the four panels of both the figures we show the expected events in five years as a function of γ . Each panel is for a certain fixed value of L , shown in the corresponding panel. In Fig. 3 the black hatched area shows the band for normal hierarchy (NH) while the open band delimited by the dashed red lines are for the inverted hierarchy (IH). As in Fig. 2 the band correspond to the uncertainty in the event rate due to the unknown δ_{CP} . The effect of the uncertainty of δ_{CP} almost vanishes for $L = 7500$ km which is very close to the magic baseline. We can see that for the smaller baseline $L = 1000$ km, NH and IH predictions are largely overlapping, making it almost impossible for these experiments to give sensitivity to the mass hierarchy unless $\sin^2 2\theta_{13}$ turns out to be extremely large and δ_{CP} favorable. The hierarchy sensitivity is expected to improve as we go to larger baselines and this is reflected from the two bands for NH and IH separating out. It turns out that because the matter effects are very large for the magic baseline and effect of CP uncertainty is zero, this baseline gives the best sensitivity to the mass hierarchy. For L larger than magic, matter effects are higher but the flux is lower, while for L lower than magic, flux is higher but the matter effects are lower. For both above and

⁴Unless stated otherwise these are the reference luminosities in all the figures. Also, all figures correspond to a five year run.

below the magic baseline, the effect of δ_{CP} is expected to further reduce the sensitivity. This is particularly true for the lower L baselines. Fig. 4 shows the bands for NH but with two different choices for $\sin^2 2\theta_{13}$. Here the effect of the magic baseline is seen even more clearly.

In Fig. 5 we show as a function of γ , the number of events expected in five years in the CERN-INO beta-beam set-up. The solid (dashed) lines are for neutrino (antineutrino) events, with the thick line showing the event rate for NH (IH) while the thin line is for the IH (NH). We have assumed $\sin^2 2\theta_{13} = 0.01$ and $\delta_{CP} = 0$. One point which is transparent from this figure and which will be very relevant in understanding the behavior of the CERN-INO beta-beam set-up is the following: For a given value of θ_{13} and for NH (IH), we expect a large number of events in the neutrino (antineutrino) channel and almost negligible events in the antineutrino (neutrino) channel. This means that for NH (IH) it will be the neutrino (antineutrino) channel which will be statistically more important.

As discussed in detail in [19] we expect hardly any background events in the CERN-INO beta-beam experiment. The atmospheric neutrino flux falls steeply with energy and is expected to produce much fewer events for the energy range that we are interested in⁵. The fact that INO has charge identification capability further reduces the atmospheric background. The most important handle on the reduction of this background comes from the timing information of the ion bunches inside the storage ring. For 5T magnetic field and $\gamma = 650$ for 8B ions, the total length of the storage ring turns out to be 19564 m. We have checked that with eight bunches inside this ring at any given time, a bunch size of about 40 ns would give an atmospheric background to *signal* ratio of about 10^{-2} , even for a very low $\sin^2 2\theta_{13}$ of 10^{-3} . For a smaller bunch span, this will go down even further. In addition, atmospheric neutrinos will be measured in INO during deadtime and this can also be used to subtract them out. Hence we do not include this negligible background here. In our numerical analysis we have assumed that the background events come only from the neutral current interactions of the beta-beam in the detector. We estimate it by assuming an energy independent background fraction of $\sim 10^{-4}$ [45]. We have noted that after five years of running of the CERN-INO beta-beam experiment with $\gamma = 650$, we expect only about 0.1 background events. Nevertheless we take this background into account in our numerical analysis. Details of our numerical analysis are given in the Appendix.

3 Measurement of the Neutrino Mass Hierarchy

In Fig. 6 we show the minimum value of $\sin^2 2\theta_{13}$ for which it would still be possible to reject the wrong hierarchy by this experimental set-up at the 3σ C.L.⁶. The left panel shows the hierarchy sensitivity when the normal hierarchy is true, while the right panel corresponds to the inverted hierarchy being true. We show this as a function of γ . In both panels we show by the red solid lines the sensitivity when we add neutrino and antineutrino data with the same value of the Lorentz boost shown in the x -axis. The blue dashed lines on the other hand correspond to the sensitivity expected when the neutrino beam runs with the γ shown in the x -axis while the γ for

⁵We will show in the next section that even a threshold energy of 4 GeV is easily admissible in our set-up, and above 4 GeV there are much fewer atmospheric events.

⁶We have given the details of our numerical analysis method in the Appendix.

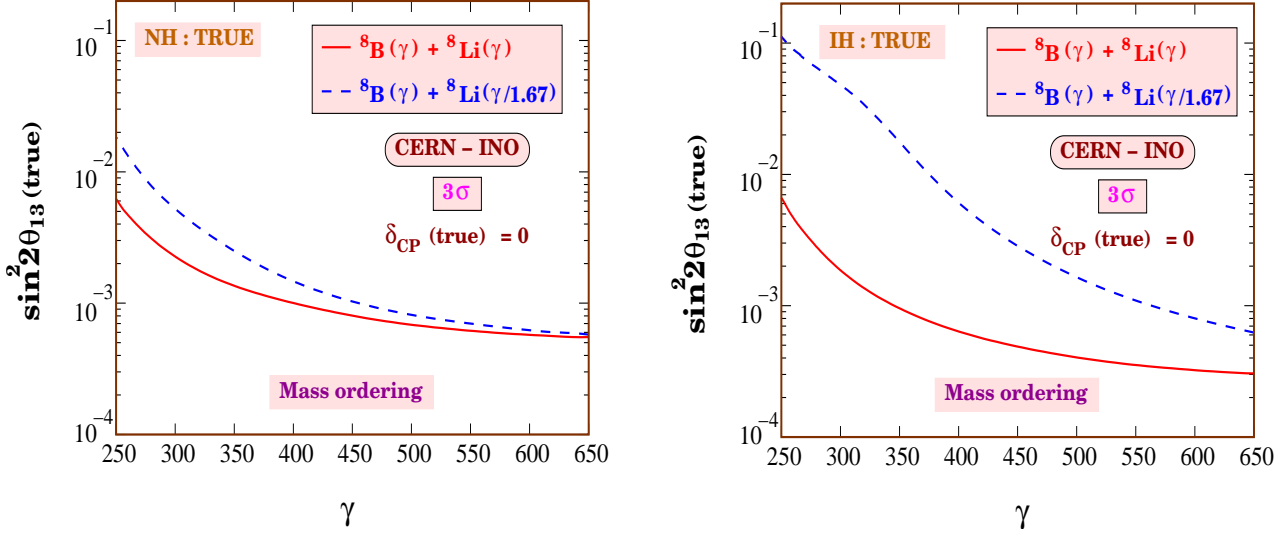


Figure 6: Minimum value of $\sin^2 2\theta_{13}(\text{true})$ for which the wrong hierarchy can be ruled out at the 3σ C.L., as a function of γ . The left panel is for normal hierarchy as true, while the right panel is when inverted hierarchy is true. The red solid curves show the sensitivity when the γ is chosen to be the same for both the neutrino and the antineutrino beams. The blue dashed lines show the corresponding sensitivity when the γ for the antineutrinos is scaled down by a factor of 1.67 with respect to the γ of the neutrino beam.

the antineutrino beam is scaled down by a factor of 1.67. We assume five years of running of the beta-beam in both polarities and we have performed a full spectral analysis. We note that using the combined neutrino and antineutrino beam running at the same value of γ significantly enhances the hierarchy sensitivity of the experiment and the wrong hierarchy could be ruled out at 3σ for $\sin^2 2\theta_{13} > 6.8 \times 10^{-4}$ ($\sin^2 2\theta_{13} > 4.0 \times 10^{-4}$) for $\gamma = 500$ if the normal (inverted) hierarchy is true. This should be compared to the results from our earlier paper where we demonstrated that by using the beam with a single polarity, the wrong hierarchy can be rejected at the 3σ C.L. for $\sin^2 2\theta_{13} > 9.8 \times 10^{-3}$ ($\sin^2 2\theta_{13} > 8.2 \times 10^{-3}$) when the normal (inverted) hierarchy is true. Partial improvement in the hierarchy sensitivity comes from the fact that we have used spectral information here, while in our earlier analysis we had considered just the total event rate measured in the detector. However, here the major improvement comes due to the addition of *both* the neutrino and antineutrino events, while in [19] we had considered events due to *either* the neutrino (for true normal hierarchy) *or* the antineutrino (for true inverted hierarchy) beam alone. Presence of both neutrino and antineutrino data simultaneously in the analysis restricts the fitted value of θ_{13} to be in a range very close to the assumed true value. For instance, for NH true, data corresponds to a large number of events for neutrinos and a small number of events for antineutrinos. When this is fitted with IH, we have a small number of events predicted for the neutrinos. In order to minimize the disparity between the data and prediction for neutrinos, the fit tends to drive θ_{13} to its largest allowed value. However, larger values of θ_{13} would give very large number of antineutrino events for IH and this would be in clear conflict with the data.

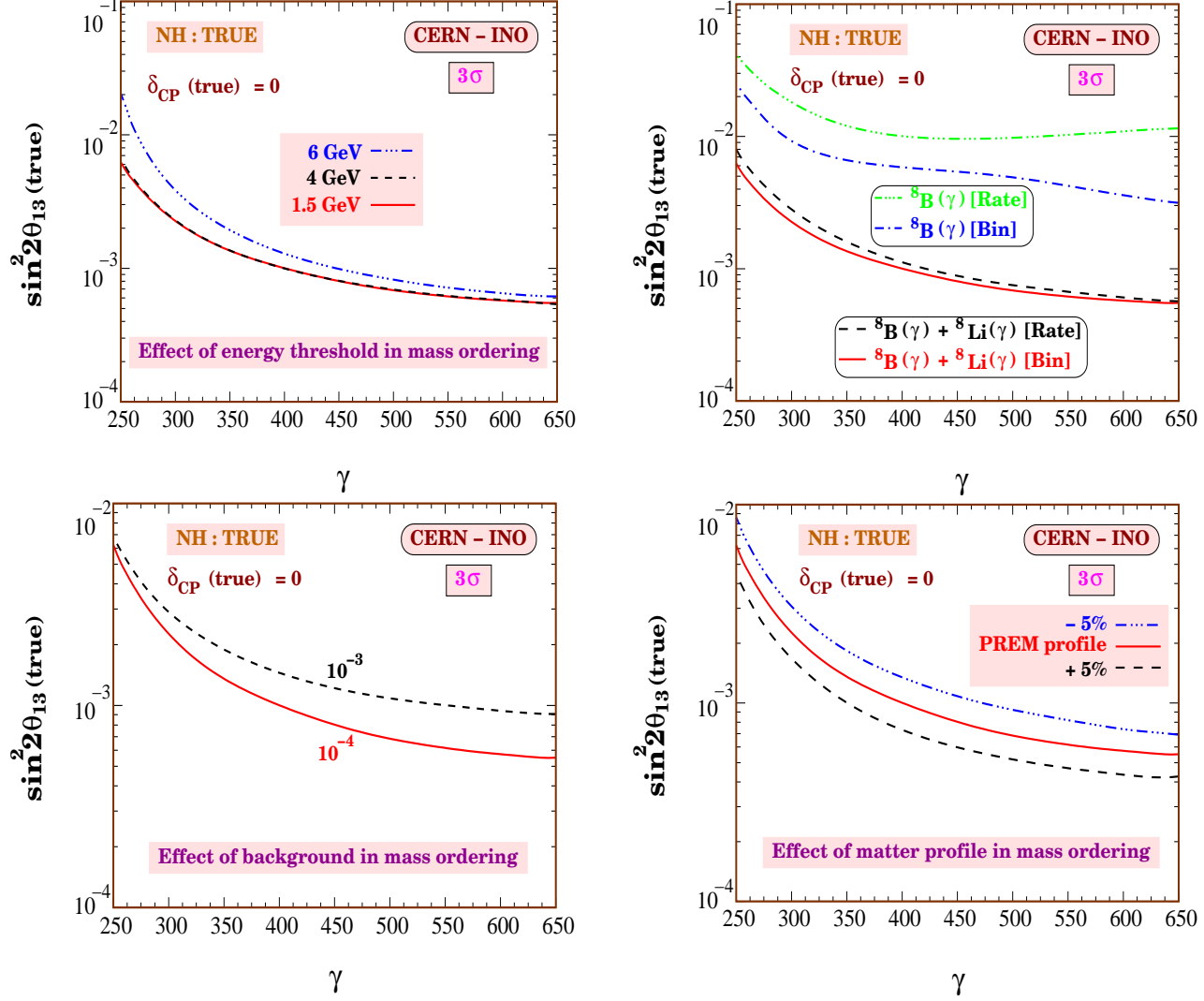


Figure 7: Plots showing the impact of various factors on the mass hierarchy sensitivity of the CERN-INO beta-beam experiment. The top left panel shows the impact of changing the detector threshold. The lower left panel shows the effect of changing the background rejection factor. The top right panel shows the difference in the sensitivity between the rate and spectral analysis. The lower right panel shows how the density profile would impact the hierarchy sensitivity.

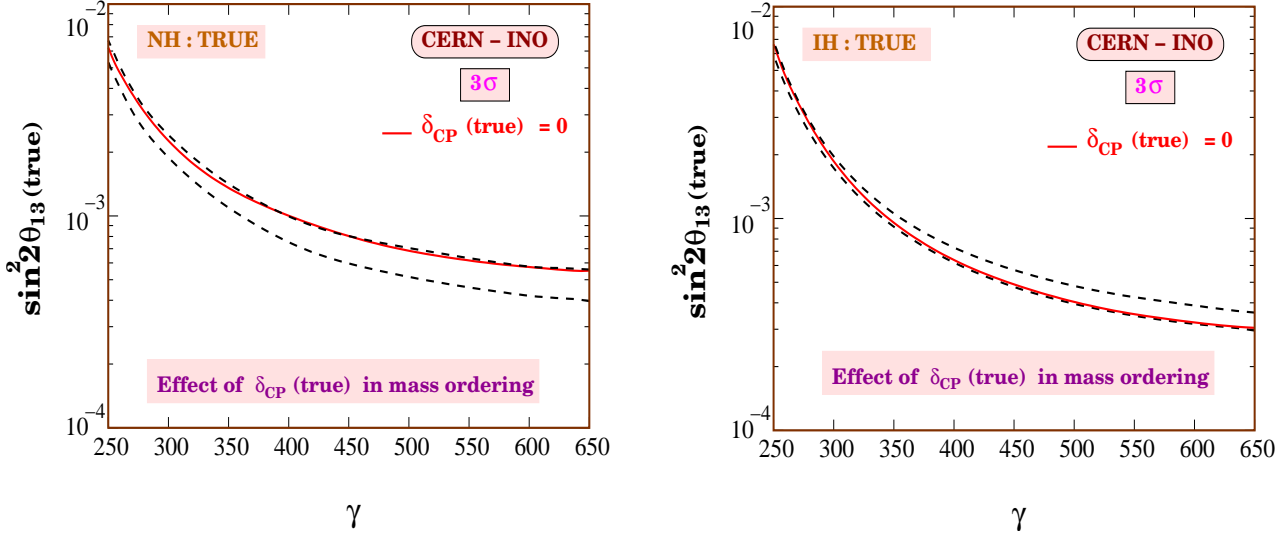


Figure 8: Effect of $\delta_{CP}(\text{true})$ on the hierarchy sensitivity. The black dashed lines show the worst and best cases when we allow $\delta_{CP}(\text{true})$ to take any value between 0 and 2π . The red solid curve corresponds to the reference case where $\delta_{CP}(\text{true}) = 0$. The left panel shows the case for true normal hierarchy while the right panel is for true inverted hierarchy.

Therefore, the net advantage of adding data from both neutrino and antineutrino channels is that one cannot artificially reduce the χ^2 any longer by tinkering with θ_{13} in the fit. As a result, the sensitivity of the experiment to mass hierarchy witnesses a substantial improvement.

We note from the plots that the hierarchy sensitivity falls when we use the scaled γ option for the antineutrino beam. This is particularly relevant when the true hierarchy is inverted and/or when γ is low. Since scaling the γ reduces it by a factor of 1.67, the statistics for the antineutrinos fall by nearly a factor of 1.67 for this case and this reflects in the reduced hierarchy sensitivity of the experiment. Its impact when true hierarchy is inverted is more because in that case, the data corresponds to larger events for the antineutrinos and very small events for the neutrinos. The antineutrino events are therefore the driving force and an increase in their statistical uncertainty due to the scaled down γ accentuates the adverse effect on the hierarchy sensitivity. In the case of normal hierarchy, the events in the neutrino channel are the dominant factor and the role of the antineutrinos is only to prevent the θ_{13} values in the fit to run to very large values, as discussed before. As long as the antineutrino events have enough statistical power to restrict θ_{13} to values close to the true value at which the data was generated, the hierarchy sensitivity remains reasonably good. Therefore, for the normal hierarchy only for very low values of γ the hierarchy sensitivity gets seriously affected by the Lorentz boost scaling.

In Fig. 7 we show how the hierarchy sensitivity depends on diverse input factors. As in Fig. 6 we show the 3σ limit for $\sin^2 2\theta_{13}$ as a function of γ in all the four panels and we assume that normal hierarchy is true. The reference curve (red solid line) in all panels corresponds to the result obtained with a ν_e and $\bar{\nu}_e$ beam with a spectral analysis. The upper left hand panel shows the effect of changing the threshold energy of the detector. The sensitivity of the experiment is seen to remain almost stable against the variation of the threshold energy upto 4 GeV. Only for a

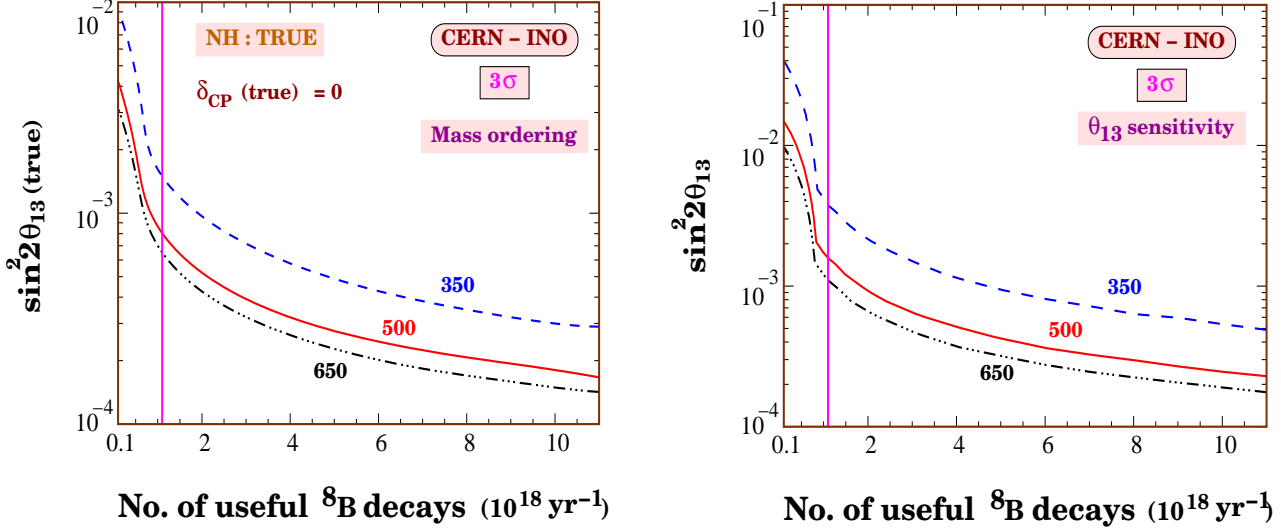


Figure 9: The variation of the experimental sensitivity on the number of useful ion decays in the straight sections of the storage ring. Left panel shows sensitivity to the mass hierarchy assuming NH to be true. Right panel shows the $\sin^2 2\theta_{13}$ sensitivity reach. In both panels, the magenta solid vertical line corresponds to the reference value used in the rest of the analysis.

threshold of 6 GeV and above the sensitivity falls, the lower γ values getting more affected since they correspond to lower neutrino energies. In the lower left hand panel of the figure we show the effect of the chosen background fraction on the hierarchy sensitivity. The red solid line shows the sensitivity for our assumed background factor of 10^{-4} while the black dashed line shows the corresponding sensitivity when the background rejection is poorer and we have a higher residual background fraction of 10^{-3} . The upper right hand panel shows how our sensitivity increases by taking into account the spectral information of the events. It also shows how much improvement we get by combining the antineutrino data with the neutrino data. The black dashed line shows how the sensitivity falls when we use the total event rates instead of the events spectrum. The blue dashed-dotted and green dashed-triple-dotted lines show the sensitivity expected from the neutrino data alone. The blue dashed-dotted line is for binned neutrino data while the green dashed-triple-dotted lines shows the sensitivity for the total event rate for neutrinos alone. We see that the effect of using the spectral information is only marginal when both neutrino and antineutrino are used, while the effect of combining the antineutrino data with the neutrino data on the sensitivity is huge. For the neutrino data alone, the sensitivity improves significantly when one uses the spectral information. In the lower right hand panel we show how the sensitivity of the experiment to hierarchy would get affected if we use a different profile for the Earth matter density instead of PREM. The red solid line is for earth density according to the PREM profile while the blue dotted and black dashed lines are when the matter density is 5% lower and 5% higher respectively than the density predicted by the PREM profile. When the density is higher (lower) the matter effects are higher (lower) and therefore the sensitivity improves (deteriorates).

One crucial point that we have not stressed so far concerns the dependence of the detector performance on the *true value* of δ_{CP} . All the earlier plots were presented assuming that

$\gamma \backslash N$	Mass Hierarchy (3σ)		$\sin^2 2\theta_{13}$ sensitivity (3σ)	
	1.1×10^{18}	2.043×10^{18}	1.1×10^{18}	2.043×10^{18}
350	1.3×10^{-3}	9.3×10^{-4}	3.8×10^{-3}	2.3×10^{-3}
650	5.6×10^{-4}	4.1×10^{-4}	1.1×10^{-3}	7.3×10^{-4}

Table 1: Comparison of the variation of the detector sensitivity to mass hierarchy (columns 2 and 3) and $\sin^2 2\theta_{13}$ sensitivity (columns 4 and 5) with γ and N , the number of useful ion decays per year.

$\delta_{CP}(\text{true}) = 0$. At exactly the magic baseline, we expect the sensitivity of the experiment to be completely independent of δ_{CP} . The CERN-INO distance of 7152 km is almost magical, but it is not the exact magic baseline. Therefore, we do expect some remnant impact of $\delta_{CP}(\text{true})$ on our results⁷. To show how our results get affected by $\delta_{CP}(\text{true})$, we show in Fig. 8 the hierarchy sensitivity just as in Fig. 6, but here we show the full band corresponding to all values of $\delta_{CP}(\text{true})$ from 0 to 2π . As before, the left panel is for NH true while the right panel is for IH true, and we have taken in the analysis the full spectral data for the neutrinos as well as the antineutrinos, with the same γ . The lower edge of this band shows the best possible scenario where the experiment is most sensitive, while the upper edge shows the worst possible sensitivity. The red solid lines in both panels show for comparison the hierarchy sensitivity corresponding to $\delta_{CP}(\text{true}) = 0$, which we had presented in Fig. 6. We note from the figure that the hierarchy sensitivity is nearly the best for $\delta_{CP}(\text{true}) = 0$ when IH is true while if NH is true then it would give us almost the worst sensitivity. For NH (IH) as true the best possible sensitivity would be $\sin^2 2\theta_{13} > 3.96 \times 10^{-4}$ ($\sin^2 2\theta_{13} > 2.96 \times 10^{-4}$) for $\gamma = 650$ to be compared with $\sin^2 2\theta_{13} > 5.51 \times 10^{-4}$ ($\sin^2 2\theta_{13} > 3.05 \times 10^{-4}$) when $\delta_{CP}(\text{true}) = 0$. Therefore, we conclude that if NH is true then it would not be unfair to expect an even better hierarchy sensitivity than what was reported in Fig. 6, while if IH is true then the best sensitivity will be returned for $\delta_{CP}(\text{true}) \simeq 0$.

We have noted from Figs. 3 and 4 that the total number of events in the detector increases roughly linearly with γ , except for extremely long baselines. Increasing the number of ion decays per year will also bring about a simple linear increase in the statistics. It is therefore pertinent to make a fair comparison between the dependence of the mass hierarchy sensitivity to the Lorentz boost γ and the number of useful ion decays in the ring⁸. In the left panel of Fig. 9 we show the effect of increasing the number of ion decays on the hierarchy sensitivity⁹. The plots exhibit the

⁷Note that in all our results presented in this paper, we have fully marginalized over all the oscillation parameters in the fit, including δ_{CP} .

⁸Note that this is also equivalent to increasing the total exposure time of the experiment. Both number of ion decays per year and exposure appear as a normalization factor for the event rate and hence increasing the number of ion decays by a factor n keeping the exposure same is equivalent to increasing the exposure by a factor n keeping the number of ion decays per year fixed.

⁹We assume that the number of useful ion decays for both 8B and 8Li have been scaled by the same factor. In the figure along the x -axis only the 8B numbers are shown.

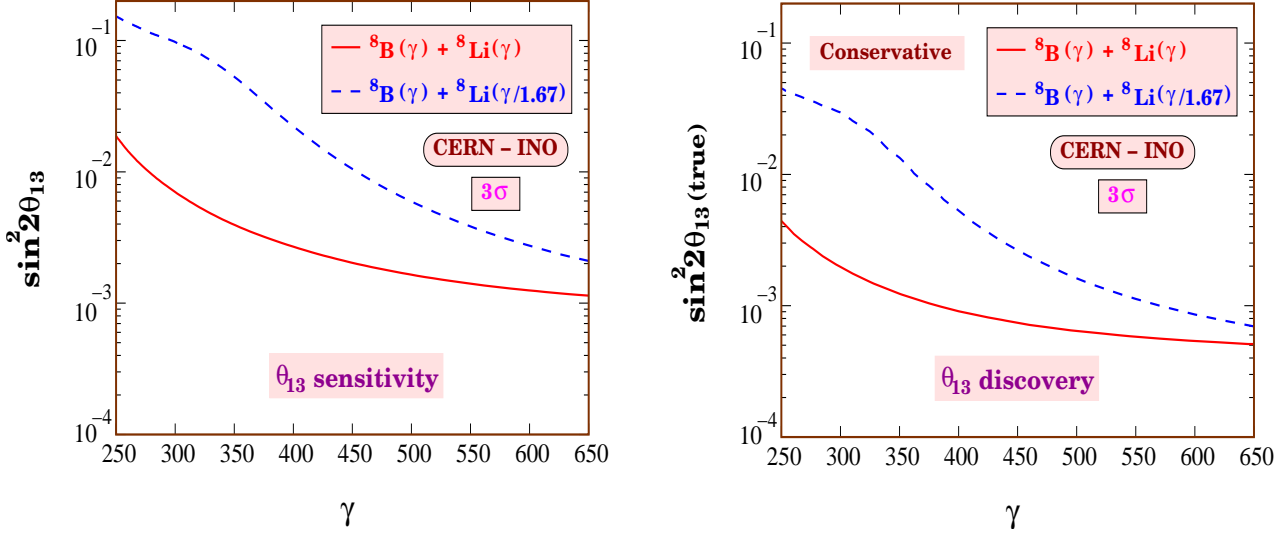


Figure 10: Left panel shows the 3σ sensitivity limit for $\sin^2 2\theta_{13}$. Right panel shows the 3σ discovery reach for $\sin^2 2\theta_{13}(\text{true})$. The red solid lines in the left and right panels show the sensitivity reach and discovery potential respectively, when the γ is assumed to be the same for both the neutrino and the antineutrino beams. The blue dashed lines show the corresponding limits when the γ for the ${}^8\text{Li}$ is scaled down by a factor of 1.67 with respect to the γ of the neutrino beam, which is plotted in the x -axis.

dependence of the sensitivity on the number of useful ion decays per year for an exposure of five years, for three different values of γ . We have assumed the same Lorentz boost for the neutrino and antineutrino beams. We present in Table 1 the relative increase in the hierarchy sensitivity when we increase the γ by a factor of 1.86 and compare it against the increase in the sensitivity when the number of ion decays are increased by the same factor. We note that while the hierarchy sensitivity improves by a factor of 2.54 in going from $\gamma = 350$ to 650 keeping the number of ion decays per year as 1.1×10^{18} , it increases 1.5-fold when we raise the number of ion decays per year from 1.1×10^{18} to 2.04×10^{18} keeping $\gamma = 350$. However, we would like to stress that the improvement of the hierarchy sensitivity is not linear with either γ or number of ion decays per year. The crucial thing is that the behavior of the sensitivity dependence on both γ and number of ion decays per year is very similar. It increases very fast initially and then comparatively flattens out.

4 Measurement of $\sin^2 2\theta_{13}$

The CERN-INO beta-beam set-up is also expected to give very good sensitivity to the θ_{13} measurement. In what follows, we will quantify our results in terms of three “performance indicators”,

1. $\sin^2 2\theta_{13}$ sensitivity reach,
2. $\sin^2 2\theta_{13}$ discovery reach,

3. $\sin^2 2\theta_{13}$ precision.

We give below a detailed description of our definition of these performance indicators. For all results in this section we take into account the full event spectrum and combine five years data from both the neutrino and antineutrino channels.

4.1 $\sin^2 2\theta_{13}$ Sensitivity Reach

We define the sensitivity reach of the CERN-INO beta-beam experiment as the upper limit on $\sin^2 2\theta_{13}$ that can be put at the 3σ C.L., in case no signal for θ_{13} driven oscillations is observed and the data is consistent with the null hypothesis. We simulate this situation in our analysis by generating the data at $\sin^2 2\theta_{13}(\text{true}) = 0$ and fitting it with some non-zero value of $\sin^2 2\theta_{13}$ by means of the χ^2 technique. In our fit we marginalize over all the oscillation parameters including δ_{CP} and further marginalize over the mass hierarchy¹⁰ and choose the value of $\sin^2 2\theta_{13}$ for which the fit yields $\chi^2 = 9$. The result is shown in the left panel of Fig. 10, as a function of γ . The red solid line shows the $\sin^2 2\theta_{13}$ sensitivity when γ is assumed to be the same for both the neutrino and the antineutrino beams. The blue dashed lines show the corresponding 3σ upper limit when γ for the ${}^8\text{Li}$ is scaled down by a factor of 1.67 with respect to that for the neutrino beam. We can compare our results here with those obtained from our earlier analysis in [19] where we had considered data from either the neutrino or the antineutrino channel alone when the hierarchy was normal and inverted, respectively. We find that the $\sin^2 2\theta_{13}$ we obtain from the combined neutrino and antineutrino data does not exhibit any marked improvement compared to that obtained in [19]. This can be understood by the following reasoning. In generating the data we have assumed that $\sin^2 2\theta_{13}(\text{true}) = 0$, which means that we have negligible events in both the neutrino as well as the antineutrino channels, irrespective of the mass hierarchy. When this data is fitted allowing for non-zero $\sin^2 2\theta_{13}$, the neutrino (antineutrino) channel plays a dominating role when NH (IH) is assumed in the fit. Therefore, the sensitivity we obtain assuming NH (IH) in our fit is similar to what we had in [19] for the neutrino (antineutrino) channel alone. However, we reiterate that Fig. 10 shows the $\sin^2 2\theta_{13}$ sensitivity after marginalizing over hierarchy as well. In other words, the sensitivity shown in this figure corresponds to the statistically weaker channel. For the case where we use same γ for ${}^8\text{B}$ and ${}^8\text{Li}$, the neutrino channel is weaker since the event rate is about 1.5 times less than antineutrino events with the same γ . On the other hand when we scale down the Lorentz boost for ${}^8\text{Li}$, the flux in the antineutrino channel goes down significantly and hence it becomes the statistically weaker channel as can be seen from Fig. 5 and therefore the marginalized χ^2 corresponds mainly to that from antineutrinos. Indeed one can check that the $\sin^2 2\theta_{13}$ sensitivity that we exhibit by the blue dashed line for the scaled γ case is comparable to what we had obtained for the antineutrino channel with IH and the corresponding lower γ .

The dependence of the $\sin^2 2\theta_{13}$ sensitivity on the number of useful radioactive ion decays per year in the straight section of the storage ring is shown in the right panel of Fig. 9. Here we have taken the same Lorentz boost for ${}^8\text{B}$ and ${}^8\text{Li}$ and we have shown the results for three fixed

¹⁰Note that since $\sin^2 2\theta_{13}(\text{true}) = 0$, the data is independent of the mass hierarchy. However, since we allow for non-zero $\sin^2 2\theta_{13}$ in the fit, the predicted event rates in our “theory” depend on the mass hierarchy.

values of γ . The relative increase in the sensitivity by increasing γ and/or the number of useful ion decays per year by the same factor is quantified in the last two columns of Table 1.

4.2 $\sin^2 2\theta_{13}$ Discovery Reach

How good are our chances of observing a positive signal for oscillations and hence θ_{13} in the CERN-INO beta-beam set-up? We answer this question in terms of the parameter indicator which we call the “discovery reach” of the experiment for $\sin^2 2\theta_{13}$. This is the minimum value of $\sin^2 2\theta_{13}(\text{true})$ that would give an unambiguous signal in the detector at 3σ . To find this we simulate the data at some non-zero value of $\sin^2 2\theta_{13}(\text{true})$ and fit it by assuming that $\sin^2 2\theta_{13} = 0$, allowing all other oscillations parameters to take any possible value in order to return back the smallest value for the χ^2 . Note that since the fitted value of the mixing angle in this case always corresponds to 0, there is no need of any marginalizing over the hierarchy when fitting the data. However, since the data here is generated at a non-zero value of $\sin^2 2\theta_{13}(\text{true})$, it depends on the true mass hierarchy. The discovery reach of the experiment is therefore expected to be dependent on the true mass hierarchy. Likewise, while the value of δ_{CP} in the fit is inconsequential as $\sin^2 2\theta_{13} = 0$ in the fit, the data itself and hence the discovery reach, would depend on $\delta_{CP}(\text{true})$. For each $\sin^2 2\theta_{13}(\text{true})$, we generate the data for all possible values of $\delta_{CP}(\text{true})$ and for both the mass hierarchies. For each case, the data is then fitted assuming $\sin^2 2\theta_{13} = 0$ and marginalizing over the other oscillation parameters, returning a value of χ^2_{\min} for each data set. We choose the minimum amongst these χ^2_{\min} and find the value of $\sin^2 2\theta_{13}(\text{true})$ for which we could claim a signal in the detector at the 3σ C.L. In the right panel of Fig. 10 we show this “most conservative”¹¹ $\sin^2 2\theta_{13}$ discovery reach of our experiment as a function of γ . We assume equal γ for both the ions for the red solid curve. One can see that for $\gamma = 650$, the most conservative discovery reach is $\sin^2 2\theta_{13}(\text{true}) = 5.11 \times 10^{-4}$ while if $\delta_{CP}(\text{true}) = 0$ then this will be $\sin^2 2\theta_{13}(\text{true}) = 5.05 \times 10^{-4}$. For the blue dashed line we assume that the γ for ${}^8\text{Li}$ is scaled down by a factor of 1.67 compared to that for ${}^8\text{B}$, plotted on the x -axis. Since for same γ , neutrino is the statistically weaker channel, the red line mainly corresponds to what we expect for the true NH. For the scaled γ case since the antineutrino channel becomes statistically weaker, the lower χ^2 comes from this channel and the blue dashed line corresponds to what we expect for the true IH.

4.3 $\sin^2 2\theta_{13}$ Precision

In Fig. 11 we show how *precisely* the mixing angle $\sin^2 2\theta_{13}$ will be measured, if we observe a θ_{13} driven signal at the detector. The left panel depicts as a function of $\sin^2 2\theta_{13}(\text{true})$ the corresponding range of allowed values of $\sin^2 2\theta_{13}$ at the 3σ C.L. We have assumed $\gamma = 500$ and $\delta_{CP} = 0$. The solid line is assuming NH to be true, while the dashed line is for IH true. Note that in the fit we always marginalize over the hierarchy and δ_{CP} . The right panel shows the variable

¹¹This is “most conservative” in the sense that no matter what the choices of $\delta_{CP}(\text{true})$ and the true neutrino mass ordering, the θ_{13} discovery limit cannot be worse than the value presented.

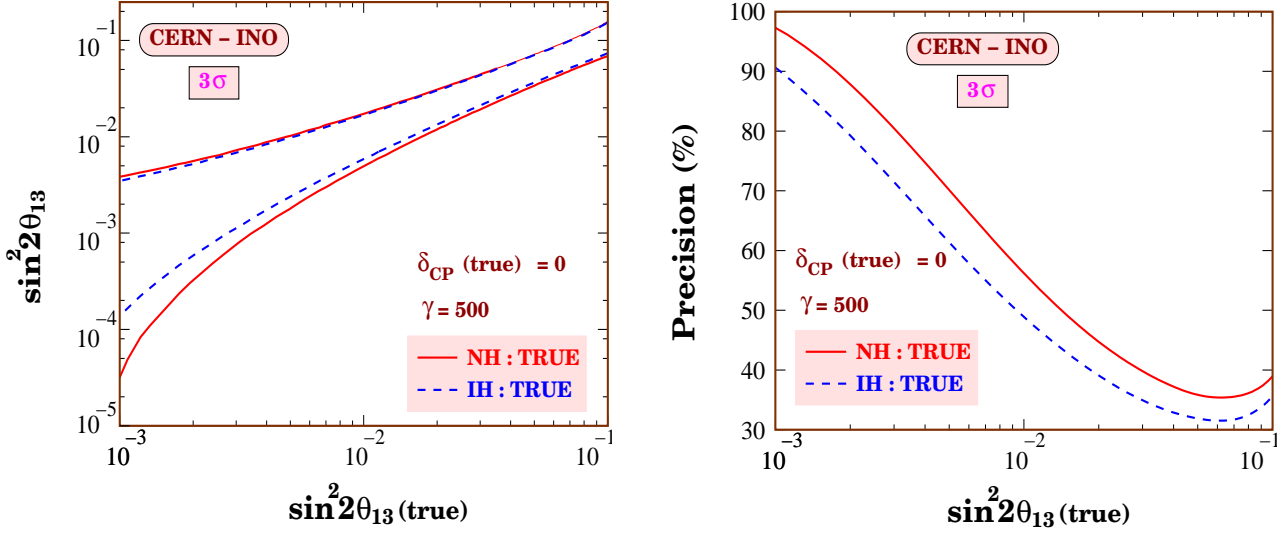


Figure 11: The precision with which $\sin^2 2\theta_{13}$ will be measured by the CERN-INO beta-beam experiment as a function of $\sin^2 2\theta_{13}(\text{true})$. Left panel shows the 3σ allowed range of $\sin^2 2\theta_{13}$ while the right panel shows the precision defined in the text.

“precision” which we define as

$$\text{precision} = \frac{(\sin^2 2\theta_{13})_{\max} - (\sin^2 2\theta_{13})_{\min}}{(\sin^2 2\theta_{13})_{\max} + (\sin^2 2\theta_{13})_{\min}} \times 100\% , \quad (4)$$

where $(\sin^2 2\theta_{13})_{\max}$ and $(\sin^2 2\theta_{13})_{\min}$ are the maximum and minimum allowed values of $\sin^2 2\theta_{13}$ respectively at 3σ .

5 Conclusions

Long baseline experiments which will use the golden $P_{e\mu}$ channel for determining the neutrino oscillation parameters face a serious threat from the menace of clone solutions due to the so-called parameter degeneracies. These degeneracies come in three forms: the $\delta_{CP} - \theta_{13}$ intrinsic degeneracy, the $\delta_{CP} - \text{sgn}(\Delta m_{31}^2)$ degeneracy and the θ_{23} octant degeneracy, and necessarily result in degrading the sensitivity of the experiment. The CERN-INO near-magic distance of 7152 km offers the possibility of setting up an experiment at a baseline where the δ_{CP} dependent terms almost drop out from the expression of the golden channel probability. Thus two out of the three degeneracies are evaded, providing a platform for clean measurement of θ_{13} and $\text{sgn}(\Delta m_{31}^2)$, two major players in our understanding of the origin of neutrino masses and mixing. A large magnetized iron calorimeter with a total mass of at least 50 kton is expected to be built soon at INO. It will be ideal for detecting multi-GeV ν_μ and hence can be used as the far detector for a high energy beta-beam.

In this paper we studied in detail the physics reach of the CERN-INO magical beta-beam set-up and extended our analysis presented in [19]. Most importantly, we showed the impact of

adding data from both the neutrino and antineutrino runs of the experiment. Combined data from both the neutrino and antineutrino polarities brings a major improvement in the hierarchy sensitivity of the experiment. We took into account the uncertainty due the solar parameters Δm_{21}^2 and $\sin^2 \theta_{12}$ and marginalized the χ^2 over them. We also accounted for the uncertainty in the Earth matter density profile in our χ^2 fit. We studied the impact of changing the energy threshold and the background rejection factor of the detector. We probed the importance of using the full spectral information on the final sensitivity of the experiment. For $\gamma = 650$, $\delta_{CP}(\text{true}) = 0$ and true NH, the sensitivity to hierarchy determination at 3σ improves almost two orders of magnitude from $\sin^2 2\theta_{13}(\text{true}) = 1.15 \times 10^{-2}$ for the neutrino channel using the total rate only to $\sin^2 2\theta_{13}(\text{true}) = 5.51 \times 10^{-4}$ when full spectral data from neutrino and antineutrino channels are combined. Even though the effect of $\delta_{CP}(\text{true})$ on the event rate of our experiment is expected to be small, there is some residual dependence on it because the CERN-INO distance does not conform to the exact magic baseline. We studied the change in the hierarchy sensitivity due to the uncertainty in δ_{CP} . It turns out that for $\gamma = 650$ and with NH (IH) true, the best sensitivity to hierarchy determination corresponds to $\sin^2 2\theta_{13}(\text{true}) = 3.96 \times 10^{-4}$ ($\sin^2 2\theta_{13}(\text{true}) = 2.96 \times 10^{-4}$), while the worst case is $\sin^2 2\theta_{13}(\text{true}) = 5.58 \times 10^{-4}$ ($\sin^2 2\theta_{13}(\text{true}) = 3.59 \times 10^{-4}$).

We presented a detailed analysis of the potential of probing θ_{13} at this experiment. We defined and studied the θ_{13} reach in terms of three performance indicators: the sensitivity reach, the discovery reach and the precision of $\sin^2 2\theta_{13}$ measurement. The sensitivity reach is defined as the upper limit on $\sin^2 2\theta_{13}$ that we would be able to impose in case the data is consistent with null oscillations. At 3σ C.L. the sensitivity reach corresponds to $\sin^2 2\theta_{13} = 1.14 \times 10^{-3}$ for $\gamma = 650$ and this is independent of the true hierarchy and $\delta_{CP}(\text{true})$. The discovery reach is defined as the true value of the mixing angle for which we have an unambiguous oscillation signal in the detector. At 3σ C.L. the discovery reach corresponds to $\sin^2 2\theta_{13}(\text{true}) = 5.05 \times 10^{-4}$ ($\sin^2 2\theta_{13}(\text{true}) = 2.96 \times 10^{-4}$) for $\gamma = 650$, $\delta_{CP}(\text{true}) = 0$ and NH (IH) true while the most conservative limit irrespective of $\delta_{CP}(\text{true})$ and the true neutrino mass ordering is $\sin^2 2\theta_{13}(\text{true}) = 5.11 \times 10^{-4}$. We also presented the expected precision with which $\sin^2 2\theta_{13}$ would be determined in this experiment for $\sin^2 2\theta_{13}(\text{true}) > 10^{-3}$.

Neutrino physics is in wait for the next great leap forward in the decade ahead. Beta-beams and an iron calorimeter detector at a very long baseline may well turn out, as we have demonstrated, to be a key player in this endeavour.

Acknowledgments

We are grateful to A. Samanta for providing us with the simulated number of atmospheric events expected in INO. We thank W. Winter for helpful discussions, and acknowledge the HRI cluster facilities for computation. This work has been supported by the XIth Plan Neutrino Project of the Harish-Chandra Research Institute.

Appendix: The Numerical Analysis

In this appendix, we give more details of our numerical technique through which we statistically explore the physics potential of our set up. The ν_μ induced μ^- event spectrum at INO is estimated

using

$$N_i = T n_n f_{ID} \epsilon \int_0^{E_{\max}} dE \int_{E_A^{\min}}^{E_A^{\max}} dE_A \phi(E) \sigma_{\nu_\mu}(E) R(E, E_A) P_{e\mu}(E) \quad (5)$$

where N_i are the number of events in energy bin i with lower energy limit E_A^{\min} and upper energy limit E_A^{\max} , T is the exposure time, n_n are the number of target nucleons, f_{ID} is the charge identification efficiency, ϵ is the detection efficiency, $\phi(E)$ is the beta-beam flux at INO, σ_{ν_μ} is the detection cross section for ν_μ , $R(E, E_A)$ is the detector energy resolution function¹², E being the true energy of the incoming neutrino and E_A the measured energy of the muon. The corresponding μ^+ spectrum due to $\bar{\nu}_\mu$ is given by replacing ϕ_{ν_e} by $\phi_{\bar{\nu}_e}$, σ_{ν_μ} by $\sigma_{\bar{\nu}_\mu}$ and $P_{e\mu}$ by $P_{\bar{e}\bar{\mu}}$ in Eq. (5). We have used $f_{ID} = 0.95$, $\epsilon = 0.8$ and taken the neutrino-nucleon interaction cross sections from [46, 47, 48]. In this paper we consider only the neutral current backgrounds coming from the beam itself. We assume that the background can be rejected very efficiently by imposing suitable cuts such that only a fraction of 10^{-4} of these neutral current backgrounds survive. The background is assumed to have the same shape as the signal. But one should keep in mind the fact that this shape is not much of an issue since anyway the background is very small.

For our statistical analysis we employ a χ^2 function defined as

$$\chi_{total}^2 = \chi_{\nu_e \rightarrow \nu_\mu}^2 + \chi_{\bar{\nu}_e \rightarrow \bar{\nu}_\mu}^2 + \chi_{prior}^2, \quad (6)$$

where the first term is the contribution from the neutrino channel, the second term comes from the antineutrino channel, while the last term comes from imposing priors on the oscillation parameters which we allow to vary freely in our fit and which we expect will be determined better from other experiments at the time when the data from the CERN-INO beta-beam set-up would be finally available. The χ^2 for the neutrino channel is given by

$$\chi_{\nu_e \rightarrow \nu_\mu}^2 = \min_{\xi_s, \xi_b} \left[2 \sum_{i=1}^n (\tilde{y}_i - x_i - x_i \ln \frac{\tilde{y}_i}{x_i}) + \xi_s^2 + \xi_b^2 \right]. \quad (7)$$

where n is the total number of bins,

$$\tilde{y}_i(\{\omega\}, \{\xi_s, \xi_b\}) = N_i^{th}(\{\omega\}) [1 + \pi^s \xi_s] + N_i^b [1 + \pi^b \xi_b], \quad (8)$$

$N_i^{th}(\{\omega\})$ given by Eq. (5) being the predicted number of events in the energy bin i for a set of oscillation parameters ω and N_i^b are the number of background events in bin i . The quantities π^s and π^b in Eq. (8) are the systematical errors on signals and backgrounds respectively. We have taken $\pi^s = 2.5\%$ and $\pi^b = 5\%$. The quantities ξ_s and ξ_b are the “pulls” due to the systematical error on signal and background respectively. The data in Eq. (7) enters through the variables $x_i = N_i^{ex} + N_i^b$, where N_i^{ex} are the number of observed signal events in the detector and N_i^b is the background, as mentioned earlier. We simulate the signal event spectrum using Eq. (5) for our assumed true values for the set of oscillation parameters. These assumed true values are given in the first column of Table 2. For $\sin^2 2\theta_{13}(\text{true})$, $\delta_{CP}(\text{true})$ and the true hierarchy we use different

¹²We assume a Gaussian resolution function with $\sigma = 0.15E$.

$ \Delta m_{31}^2(\text{true}) = 2.5 \times 10^{-3} \text{ eV}^2$	$\sigma(\Delta m_{31}^2) = 1.5\%$
$\sin^2 2\theta_{23}(\text{true}) = 1.0$	$\sigma(\sin^2 2\theta_{23}) = 1\%$
$\Delta m_{21}^2(\text{true}) = 8.0 \times 10^{-5} \text{ eV}^2$	$\sigma(\Delta m_{21}^2) = 2\%$
$\sin^2 \theta_{12}(\text{true}) = 0.31$	$\sigma(\sin^2 \theta_{12}) = 6\%$
$\rho(\text{true}) = 1 \text{ (PREM)}$	$\sigma(\rho) = 5\%$

Table 2: Chosen benchmark values of oscillation parameters and their 1σ estimated error. The last row gives the corresponding values for the Earth matter density.

options and mention them wherever applicable. In our χ^2 fit we marginalize over *all* oscillation parameters, the Earth matter density, as well as the neutrino mass hierarchy, as applicable. We do this by allowing all of these to vary freely in the fit and picking the smallest value for the χ^2 function. Of course we expect better determination of some of these parameters, which are poorly constrained by this experimental set-up. Therefore, we impose a “prior” on these parameters through the χ_{prior}^2 given by

$$\begin{aligned}
\chi_{prior}^2 = & \left(\frac{|\Delta m_{31}^2| - |\Delta m_{31}^2(\text{true})|}{\sigma(|\Delta m_{31}^2|)} \right)^2 + \left(\frac{\sin^2 2\theta_{23} - \sin^2 2\theta_{23}(\text{true})}{\sigma(\sin^2 2\theta_{23})} \right)^2 \\
& + \left(\frac{\Delta m_{21}^2 - \Delta m_{21}^2(\text{true})}{\sigma(\Delta m_{21}^2)} \right)^2 + \left(\frac{\sin^2 \theta_{12} - \sin^2 \theta_{12}(\text{true})}{\sigma(\sin^2 \theta_{12})} \right)^2 \\
& + \left(\frac{\rho - 1}{\sigma(\rho)} \right)^2 .
\end{aligned} \tag{9}$$

where the 1σ error on these that we use are taken from [16, 49] and are given in the left column of Table 2. In our computation, we have used a matter profile inside the Earth with 24 layers. In Eq. (9), ρ is a constant number by which the matter density of each layer has been scaled. The external information on ρ is assumed to come from the study of the tomography of the earth [50]. In Eq. (9), ρ varies from 0.95 to 1.05 i.e., 5% fluctuation around 1.

Note that in our definition of the χ^2 function given by Eq. (6) and (7) we have assumed that the neutrino and antineutrino channel are completely uncorrelated, all the energy bins for a given channel are fully correlated, and ξ_s and ξ_b are fully uncorrelated. We minimize the χ_{total}^2 in two stages. First it is minimized with respect to ξ_s and ξ_b to get Eq. (7), and then with respect to the oscillation parameters ω to get the global best-fit. For minima with respect to ξ_s and ξ_b , we require that

$$\frac{\partial \chi^2}{\partial \xi_s} = 0 \quad \text{and} \quad \frac{\partial \chi^2}{\partial \xi_b} = 0 . \tag{10}$$

From Eq. (7, 8, 10) we get,

$$\begin{pmatrix} a_{11} & a_{12} \\ a_{21} & a_{22} \end{pmatrix} \begin{pmatrix} \xi_s \\ \xi_b \end{pmatrix} = \begin{pmatrix} c_1 \\ c_2 \end{pmatrix} \quad (11)$$

where,

$$\begin{aligned} c_1 &= \sum_{i=1}^n \left(\frac{x_i \pi^s N_i^{th}}{N_i^{th} + N_i^b} - \pi^s N_i^{th} \right), \\ c_2 &= \sum_{i=1}^n \left(\frac{x_i \pi^b N_i^b}{N_i^{th} + N_i^b} - \pi^b N_i^b \right), \\ a_{11} &= \sum_{i=1}^n \left[\frac{x_i (\pi^s N_i^{th})^2}{(N_i^{th} + N_i^b)^2} \right] + 1, \\ a_{22} &= \sum_{i=1}^n \left[\frac{x_i (\pi^b N_i^b)^2}{(N_i^{th} + N_i^b)^2} \right] + 1, \\ a_{12} &= a_{21} = \sum_{i=1}^n \left[\frac{x_i N_i^{th} N_i^b \pi^s \pi^b}{(N_i^{th} + N_i^b)^2} \right] \end{aligned} \quad (12)$$

Using Eq. (11 and 12), we calculate the values of ξ_s and ξ_b and then we use these values to calculate $\chi_{\nu_e \rightarrow \nu_\mu}^2$. In a similar fashion, we estimate $\chi_{\bar{\nu}_e \rightarrow \bar{\nu}_\mu}^2$ to obtain the χ_{total}^2 .

References

- [1] B. T. Cleveland *et al.*, *Astrophys. J.* **496**, 505 (1998); J. N. Abdurashitov *et al.* [SAGE Collaboration], *J. Exp. Theor. Phys.* **95**, 181 (2002) [*Zh. Eksp. Teor. Fiz.* **122**, 211 (2002)]; W. Hampel *et al.* [GALLEX Collaboration], *Phys. Lett. B* **447**, 127 (1999); S. Fukuda *et al.* [Super-Kamiokande Collaboration], *Phys. Lett. B* **539**, 179 (2002); B. Aharmim *et al.* [SNO Collaboration], *Phys. Rev. C* **72**, 055502 (2005).
- [2] C. Arpesella *et al.*, [Borexino Collaboration], arXiv:0708.2251 [astro-ph].
- [3] K. Eguchi *et al.*, [KamLAND Collaboration], *Phys. Rev. Lett.* **90**, 021802 (2003); T. Araki *et al.* [KamLAND Collaboration], *Phys. Rev. Lett.* **94**, 081801 (2005).
- [4] I. Shimizu, talk at 10th International Conference on Topics in Astroparticle and Underground Physics, TAUP 2007.
- [5] M. Maltoni, T. Schwetz, M. A. Tortola and J. W. F. Valle, *New J. Phys.* **6**, 122 (2004), hep-ph/0405172 v5; S. Choubey, arXiv:hep-ph/0509217; S. Goswami, *Int. J. Mod. Phys. A* **21**, 1901 (2006); A. Bandyopadhyay, S. Choubey, S. Goswami, S. T. Petcov and D. P. Roy, *Phys. Lett. B* **608**, 115 (2005); G. L. Fogli *et al.*, *Prog. Part. Nucl. Phys.* **57**, 742 (2006).
- [6] Y. Ashie *et al.* [Super-Kamiokande Collaboration], *Phys. Rev. D* **71**, 112005 (2005).

- [7] E. Aliu *et al.* [K2K Collaboration], Phys. Rev. Lett. **94**, 081802 (2005).
- [8] D. G. Michael *et al.*, [MINOS Collaboration], Phys. Rev. Lett. **97**, 191801 (2006).
- [9] S. Pascoli, S. T. Petcov and T. Schwetz, Nucl. Phys. B **734**, 24 (2006); S. Choubey and W. Rodejohann, Phys. Rev. D **72**, 033016 (2005).
- [10] M. Apollonio *et al.*, Eur. Phys. J. C **27**, 331 (2003).
- [11] L. Wolfenstein, Phys. Rev. D **17**, 2369 (1978).
- [12] S. P. Mikheev and A. Y. Smirnov, Sov. J. Nucl. Phys. **42**, 913 (1985) [Yad. Fiz. **42**, 1441 (1985)]; S. P. Mikheev and A. Y. Smirnov, Nuovo Cim. C **9**, 17 (1986).
- [13] V. D. Barger, K. Whisnant, S. Pakvasa and R. J. N. Phillips, Phys. Rev. D **22**, 2718 (1980).
- [14] Y. Itow *et al.*, arXiv:hep-ex/0106019.
- [15] D. S. Ayres *et al.* [NOvA Collaboration], arXiv:hep-ex/0503053.
- [16] P. Huber, M. Lindner, M. Rolinec, T. Schwetz and W. Winter, Phys. Rev. D **70**, 073014 (2004) and references therein.
- [17] <http://www.hep.ph.ic.ac.uk/iss/>
- [18] S. K. Agarwalla, A. Raychaudhuri and A. Samanta, Phys. Lett. B **629**, 33 (2005).
- [19] S. K. Agarwalla, S. Choubey and A. Raychaudhuri, Nucl. Phys. B **771**, 1 (2007).
- [20] M. S. Athar *et al.* [INO Collaboration], A Report of the INO Feasibility Study, <http://www.imsc.res.in/ino/OpenReports/INOResult.pdf>
- [21] P. Zucchelli, Phys. Lett. B **532**, 166 (2002).
- [22] J. E. Campagne, M. Maltoni, M. Mezzetto and T. Schwetz, JHEP **0704**, 003 (2007).
- [23] J. Burguet-Castell, M. B. Gavela, J. J. Gómez-Cadenas, P. Hernandez and O. Mena, Nucl. Phys. B **608**, 301 (2001).
- [24] H. Minakata and H. Nunokawa, JHEP **0110**, 001 (2001).
- [25] G. L. Fogli and E. Lisi, Phys. Rev. D **54**, 3667 (1996).
- [26] V. Barger, D. Marfatia and K. Whisnant, Phys. Rev. D **65**, 073023 (2002).
- [27] P. Huber and W. Winter, Phys. Rev. D **68**, 037301 (2003).
- [28] A. Y. Smirnov, arXiv:hep-ph/0610198.
- [29] M. Freund, M. Lindner, S. T. Petcov and A. Romanino, Nucl. Phys. B **578**, 27 (2000).

- [30] A. M. Dziewonski and D. L. Anderson, *Phys. Earth Planet. Interiors* **25**, 297 (1981); S. V. Panasyuk, Reference Earth Model (REM) webpage, <http://cfauves5.harvard.edu/lana/rem/index.html>.
- [31] P. Huber, M. Lindner, M. Rolinec and W. Winter, *Phys. Rev. D* **73**, 053002 (2006).
- [32] J. Burguet-Castell, D. Casper, E. Couce, J. J. Gómez-Cadenas and P. Hernandez, *Nucl. Phys. B* **725**, 306 (2005); J. Burguet-Castell, D. Casper, J. J. Gómez-Cadenas, P. Hernandez and F. Sanchez, *Nucl. Phys. B* **695**, 217 (2004).
- [33] C. Volpe, *J. Phys. G* **34**, R1 (2007).
- [34] M. Mezzetto, *J. Phys. G* **29**, 1771 (2003); M. Mezzetto, *Nucl. Phys. Proc. Suppl.* **143**, 309 (2005); M. Mezzetto, *Nucl. Phys. Proc. Suppl.* **155**, 214 (2006).
- [35] A. Donini, E. Fernandez-Martinez, P. Migliozi, S. Rigolin and L. Scotto Lavina, *Nucl. Phys. B* **710**, 402 (2005); A. Donini, E. Fernandez, P. Migliozi, S. Rigolin, L. Scotto Lavina, T. Tabarelli de Fatis and F. Terranova, [arXiv:hep-ph/0511134](https://arxiv.org/abs/hep-ph/0511134); A. Donini, E. Fernandez-Martinez, P. Migliozi, S. Rigolin, L. Scotto Lavina, T. Tabarelli de Fatis and F. Terranova, *Eur. Phys. J. C* **48**, 787 (2006).
- [36] C. Rubbia, A. Ferrari, Y. Kadi and V. Vlachoudis, *Nucl. Instrum. Meth. A* **568**, 475 (2006); C. Rubbia, [arXiv:hep-ph/0609235](https://arxiv.org/abs/hep-ph/0609235).
- [37] Y. Mori, *Nucl. Instrum. Meth. A* **562**, 591 (2006).
- [38] A. Donini and E. Fernandez-Martinez, *Phys. Lett. B* **641**, 432 (2006).
- [39] R. Adhikari, S. K. Agarwalla and A. Raychaudhuri, *Phys. Lett. B* **642**, 111 (2006); S. K. Agarwalla, S. Rakshit and A. Raychaudhuri, *Phys. Lett. B* **647**, 380 (2007).
- [40] A. Jansson, O. Mena, S. Parke and N. Saoulidou, [arXiv:0711.1075 \[hep-ph\]](https://arxiv.org/abs/0711.1075).
- [41] A. Cervera, A. Donini, M. B. Gavela, J. J. Gómez-Cadenas, P. Hernandez, O. Mena and S. Rigolin, *Nucl. Phys. B* **579**, 17 (2000) [Erratum-ibid. *B* **593**, 731 (2001)].
- [42] M. Freund, P. Huber and M. Lindner, *Nucl. Phys. B* **615**, 331 (2001).
- [43] R. Gandhi, P. Ghoshal, S. Goswami, P. Mehta and S. Uma Sankar, *Phys. Rev. Lett.* **94**, 051801 (2005); R. Gandhi, P. Ghoshal, S. Goswami, P. Mehta and S. Uma Sankar, *Phys. Rev. D* **73**, 053001 (2006).
- [44] S. K. Agarwalla, S. Choubey, S. Goswami and A. Raychaudhuri, *Phys. Rev. D* **75**, 097302 (2007).
- [45] A. Cervera, talk at NuFact07.
- [46] P. Huber, M. Lindner and W. Winter, *Comput. Phys. Commun.* **167**, 195 (2005).

- [47] M. D. Messier, PhD thesis, UMI-99-23965.
- [48] E. A. Paschos and J. Y. Yu, Phys. Rev. D **65**, 033002 (2002).
- [49] See for example, A. Bandyopadhyay *et al.*, Phys. Rev. D **72**, 033013 (2005); J. N. Bahcall and C. Pena-Garay, JHEP **0311**, 004 (2003).
- [50] R. J. Geller and T. Hara, Nucl. Instrum. Meth. A **503**, 187 (2001).